Event-Triggered Prescribed Time Adaptive Fuzzy Fault-Tolerant Control for Nonlinear Systems With Full-State Constraints

Qingkun Yu, *Member, IAENG,* Jixin Ding, Libing Wu, and Xiqin He

***Abstract*—This work investigates the prescribed finite-time event-triggered control of uncertain nonlinear systems with full-state constraints and actuator failures. In order to approximate the unknown nonlinear dynamic function, the fuzzy logic system (FLS) is used in this paper. By integrating the backstepping design framework with Lyapunov stability theory, a novel event-triggered condition that incorporates a decreasing function of the system interstate error is proposed. The developed method not only confines tracking errors within a predetermined range within the prescribed setting time but also ensures that all states adhere to their respective constraints. Additionally, the approach effectively mitigates the impacts of the Zeno phenomenon and actuator failure. Simulation results on a mass-spring-damper system demonstrate the efficacy of the proposed method.**

***Index Terms*—event-triggered control, fault-tolerant control, prescribed finite time, barrier Lyapunov functions(BLFs), uncertain nonlinear systems.**

I. INTRODUCTION

THE theory of nonlinear systems has shown strong potential for development in recent decades. Among the key technical approaches, adaptive backstepping method [1] emerges as potent analytical tools for dealing with nonlinear systems featuring a triangular structure. In various studies, researchers commonly utilized neural networks (NNs) [2] and FLSs [3] to handle unknown items within a generalized approximation framework. The utilization of these techniques facilitates the modeling of uncertain nonlinear functions in the absence of prior knowledge. In addition, scholars have explored the application of this technique to various nonlinear systems, including strict feedback nonlinear systems [4], pure feedback nonlinear systems [5] and non-strict feedback nonlinear systems [6]. Specifically, the problem of adaptive fuzzy ETC for switch systems was focused on in [7]. FLSs are leveraged to handle unknown dynamic terms, while BLFs are employed to tackle the challenges posed by state constraints. In [8], the tracking control problem was developed by introducing a log-type time-varying BLF to prevent violations of the high-order full-state constraint. In recent years, how to reduce the communication burden in the information transfer process has become a prominent and active research issue in the evolving field of control theory.

ETC [9, 10] has gained significant attention from scholars due to its effectiveness in reducing communication burden while ensuring accurate trajectory tracking. Three distinct ETC strategies were delineated in [11]. In [12], an improved ETC strategy adapted to high order systems with predetermined performance was devised. This strategy utilized a single gain function to eliminate unknown parameters within the FLSs, resulting in a significant reduction in computational complexity for the proposed scheme. An ETC strategy incorporating an error decreasing function was proposed in [13]. Compared to traditional triggering strategies, this approach effectively reduces the number of event triggering occurrences, thus diminishing the communication burden. In addition to reducing the communication burden within a constrained network channel, ensuring convergence within a prescribed time is another key issue in practical applications.

In practice, the demand for convergence within a specified time frame is increasing. Thus, finite/fixed time stability problems have garnered significant interest, as indicated in [14, 15]. These approaches have the potential to enhance convergence speed rates compared to conventional practical tracking control methods. Fixed-time stability renders the stabilization time irrelevant to its initial conditions but relies on several design parameters. In pursuit of heightened convergence performance, prescribed-time control has emerged as a recent and fervently researched topic. This approach allows for the direct specification of a predetermined convergence time[16]. In [17], an adaptive controller was formulated with the objective of driving the system stabilisation within specified time. Besides, it should be considered that various faults can occur at any time as the system continues to operate.

Ensuring that the system maintains the expected control performance and continues to operate normally in the event of a failure is the role of fault-tolerant control. In [18], an adaptive neural containment control approach was applied to nonlinear multi-agent fault-tolerant control systems. By using backstepping method, the issue of output stabilization for multi-input and multi-output NNs with sensor and actuator faults was addressed in [19]. In [20], extension of problems with state constraints to non-affine stochastic nonlinear systems and design of fault-tolerant tracking control schemes.

Motivated by the above considerations, this paper proposes an adaptive fault-tolerant ETC scheme based on prescribed

Manuscript received January 21, 2024; revised June 14, 2024. This work was supported in part by the Natural Science Foundation of Liaoning Province (2023-MS-287).

Qingkun Yu is a doctoral student of School of Electronic and Information Engineering, University of Science and Technology Liaoning, Anshan, Liaoning, 114051, P. R. China (e-mail: yuqingkun@163.com).

Jixin Ding is a postgraduate student of School of Science, University of Science and Technology Liaoning, Anshan, Liaoning 114051, P. R. China (e-mail: dingjixin1016@126.com).

Libing Wu is a professor of School of Science, University of Science and Technology Liaoning, Anshan, Liaoning 114051, P. R. China (e-mail: beyondwlb@163.com).

Xiqin He is a professor of School of Electronic and Information Engineering, University of Science and Technology Liaoning, Anshan, Liaoning 114051, P. R. China (Corresponding author, phone: 86-412-5928444; e-mail: xiqinhe@ustl.edu.cn).

time for nonlinear systems with full-state constraints and actuator faults. The primary contributions are reflected in the following:

1) The challenges of synchronous state constraints, actuator failures and external disturbances in nonlinear systems are successfully addressed by applying backstepping and BLFs in this paper. Fault compensation is also implemented to stabilise the system.

2) A prescribed-time control strategy that allows the stabilization time and tracking accuracy to be adjusted independently is considered in this paper. Meanwhile, the settling time is irrelevant to the initial conditions.

3) A new ETC strategy is proposed, which has fewer design parameters and can reduce the communication burden compared with [7] and [13].

These contributions collectively advance the understanding and application of adaptive event-triggered fault-tolerant control in challenging nonlinear systems.

II. PROBLEM FORMULATION

Consider the uncertain nonlinear system:

$$\begin{cases} \dot{x}_i = x_{i+1} + f_i(\underline{x}_i) + d_i(t), i = \quad 1,2,\ldots,n-1, \\ \dot{x}_n = u^F + f_n(\underline{x}_n) + d_n(t), \\ y = x_1 \end{cases} \tag{1}$$

where $\underline{x}_i = [x_1, x_2, \ldots, x_i]^T \in R^i$ indicate the state vectors, and are limited by the predefined set $\mathbb{X}_i = \{x_i \in R | |x_i| < k_{c_i}\}$. f_i and $d_i(t)$ denote the unknown smooth functions and disturbances for $i = 1,2,\ldots,n$, respectively. y is the system output. u^F is the control input with the following fault model:

$$u^F(t) = \rho_a(t)u(t) + \psi(t) \tag{2}$$

where $\psi(t)$ means the additive actuator fault, and $\rho_a(t)$ denotes the multiplicative actuator fault and adheres to the condition expressed by $0 < \rho_a(t) \leqslant 1$. When $\rho_a(t) = 1$, $\psi(t) = 0$, the actuator is functioning properly.

Remark 1. The actuator fault model (2) is widely adopted in various references [21]. The additive and multiplicative actuator faults signify the introduction of extra input and the time-varying gain of the faulty actuator. It is important to note that this paper does not explore the case involving matrix $\rho_a(t) = 0$, which would lead to an underactuated system. This topic is beyond the scope of this paper.

Assumption 1 [7]: The reference signal y_d and $\dot{y}_d$ are bounded satisfying $y_d \leqslant Y_1 < k_{c_1}$.

Lemma 1 [22]: The prescribed finite-time function $\Phi(t)$ is chosen as:

$$\Phi(t) = \begin{cases} \operatorname{csch}(\nu_1 \cdot \dfrac{T_s}{T_s - t}) + \nu_2, 0 \leq t < T_s \\ \nu_2, t \geq T_s \end{cases} \tag{3}$$

where T_s, ν_1 and ν_2 are positive constants.

Lemma 2 [13]: For $\forall \varsigma \in \mathbb{R}$ and $\kappa > 0$, one has

$$0 \leq |\xi| - \xi \tanh\left(\frac{\xi}{\kappa}\right) \leq 0.2785\kappa \tag{4}$$

Next, to give Lemma 3, we present the N fuzzy IF-THEN rules:

R^i: If x_1 is F_1^i, and ... and x_n is F_n^i, then y is G^i, i=1,2,...,N.

The FLSs can be written as

$$y(x) = \frac{\sum_{i=1}^N \theta_i \prod_{j=1}^n \mu_{F_j^i}(x_j)}{\sum_{i=1}^N \prod_{j=1}^n \mu_{F_j^i}(x_j)} \tag{5}$$

choose $\theta_i = \max_{y \in R} \mu_{G^i}(y)$.

The fuzzy basis functions are described by

$$S_i(x) = \frac{\prod_{j=1}^n \mu_{F_j^i}(x_j)}{\sum_{i=1}^N \prod_{j=1}^n \mu_{F_j^i}(x_j)}. \tag{6}$$

Then (5) is given as

$$y(x) = \theta^T S(x) \tag{7}$$

where $\theta^T = [\theta_1, \theta_2, \ldots, \theta_N]$ and $S(x) = [S_1, S_2, \ldots, S_N]$.

Lemma 3 [13]: For a continuous nonlinear function $F(\underline{X})$, it has

$$\sup_{X \in \Gamma} \left| F(\underline{X}) - W^T S(\underline{X}) \right| \leq \varepsilon, \forall \varepsilon > 0 \tag{8}$$

where $W = [w_1, w_2, \ldots, w_n]^T$ is the ideal constant vector and $S(\underline{X})$ is the fuzzy basis function vector.

Lemma 4 [13]: Any $|z| < k_b$, k_b is a constant, the following result holds

$$\log \frac{k_b^2}{k_b^2 - z^2} < \frac{z^2}{k_b^2 - z^2} \tag{9}$$

Remark 2. Lemma 1 is introduced to attain prescribed finite-time stability. Lemmas 2 and 3 are utilised to address the unknown nonlinear terms during the control strategy design process. Lemma 4 plays a crucial role in conducting the Lyapunov stability analysis. For a detailed exposition of Lemmas 1-4, please refer to [13, 22] and related literature, respectively.

III. MAIN RESULTS

This subsection is to design ETC strategy with prescribed finite-time based on backstepping technique. Subsequently, the stability analysis is conducted employing the Lyapunov method.

Define the tracking error as follows

$$e = x_1 - y_d \tag{10}$$

Using Lemma 1, we then obtain

$$-T_1\Phi(t) < e(t) < T_2\Phi(t) \tag{11}$$

where $0 < T_1, T_2 < 1$.

And

$$e = \Phi(t)\Pi(\pi) \tag{12}$$

where $\Pi(\pi)$ is a smooth and strictly increasing function

$$\Pi(\pi) = \frac{T_2 e^{\pi} - T_1 e^{-\pi}}{e^{\pi} + e^{-\pi}} \tag{13}$$

Then

$$\pi(t) = \Pi^{-1}\left(\frac{e(t)}{\Phi(t)}\right) = \frac{1}{2}\ln\left(\frac{\Pi(t) + T_1}{T_2 - \Phi(t)}\right) \tag{14}$$

From (10)-(14), the following change of coordinates is defined

$$\begin{aligned} z_1 &= \pi - \frac{1}{2}\ln\frac{T_1}{T_2} \\ z_i &= x_i - \alpha_{i-1}, i = 2, \ldots, n \end{aligned} \tag{15}$$

where α_{i-1} is the virtual control.

Step 1: From (10) and (15), one has

$$\begin{aligned} \dot{z}_1 =& \varphi\left(\dot{e} - \frac{e\dot{\Phi}(t)}{\Phi(t)}\right) = \varphi\left(\dot{x}_1 - \dot{y}_d - \frac{e\dot{\Phi}(t)}{\Phi(t)}\right) \\ =& \varphi\left(z_2 + \alpha_1 + f_1 + d_1 - \dot{y}_d - \frac{e\dot{\Phi}(t)}{\Phi(t)}\right) \end{aligned} \tag{16}$$

where $\varphi = \frac{1}{2\Phi(t)}\left(\frac{1}{\Xi+T_1} + \frac{1}{T_2-\Xi}\right)$.

Consider the BLF as follows

$$V_1 = \frac{1}{2}\log\frac{k_{b1}^2}{k_{b1}^2 - z_1^2} + \frac{1}{2}\tilde{\theta}_1^2 \tag{17}$$

where $k_{b1} = k_{c1} - Y_1$, $z_1 \in \mathbb{K}_1$ and $\mathbb{K}_1 = \{z_1 || z_1| < k_{b1}\}$. $\tilde{\theta}_1 = \theta_1 - \hat{\theta}_1$, $\hat{\theta}_1$ is the estimation of θ_1.

According to (17), taking time derivative of V_1, we have

$$\dot{V}_1 \leqslant \frac{z_1\varphi}{k_{b1}^2 - z_1^2}\left(z_2 + \alpha_1 + f_1 + d_1 - \dot{y}_d - \frac{e\dot{\Phi}(t)}{\Phi(t)}\right) - \tilde{\theta}_1\dot{\hat{\theta}}_1 \tag{18}$$

From Lemma 3, one can get

$$\begin{aligned} F_1(\underline{X}_1) &= \varphi\left(f_1 + d_1 - \dot{y}_d - \frac{e\dot{\Phi}(t)}{\Phi(t)}\right) \\ &= W_1^T S_1(\underline{X}_1) + \varepsilon_1 \end{aligned} \tag{19}$$

where $\underline{X}_1 = [x_1, y_d, \dot{y}_d]^T$, $|\varepsilon_1| \leqslant \epsilon_1$, $\epsilon_1 > 0$.

Utilizing Young's inequality, one obtains

$$\begin{aligned} \frac{z_1 F_1(\underline{X}_1)}{k_{b1}^2 - z_1^2} \leqslant& \frac{z_1^2\theta_1 S_1(\underline{X}_1)^T S_1(\underline{X}_1)}{2a_1^2(k_{b1}^2 - z_1^2)^2} + \frac{a_1^2}{2} \\ &+ \frac{z_1^2}{2(k_{b1}^2 - z_1^2)^2} + \frac{\epsilon_1^2}{2} \end{aligned} \tag{20}$$

where $\theta_1 = ||W_1||^2$, and $a_1 > 0$ is a constant.

Combining (18) and (20) yields

$$\begin{aligned} \dot{V}_1 \leqslant& \frac{z_1}{k_{b1}^2 - z_1^2}\left(\varphi\alpha_1 + \frac{z_1\theta_1 S_1(\underline{X}_1)^T S_1(\underline{X}_1)}{2a_1^2(k_{b1}^2 - z_1^2)}\right. \\ &\left. + \frac{z_1}{2(k_{b1}^2 - z_1^2)}\right) + \frac{\varphi z_1 z_2}{k_{b1}^2 - z_1^2} + \frac{\epsilon_1^2}{2} + \frac{a_1^2}{2} - \tilde{\theta}_1\dot{\hat{\theta}}_1 \end{aligned} \tag{21}$$

Then, α_1 and $\hat{\theta}_1$ are constructed as

$$\alpha_1 = -\frac{1}{\varphi}\left(c_1 z_1 + \frac{z_1\hat{\theta}_1 S_1(\underline{X}_1)^T S_1(\underline{X}_1)}{2a_1^2(k_{b1}^2 - z_1^2)} + \frac{z_1}{2(k_{b1}^2 - z_1^2)}\right) \tag{22}$$

$$\dot{\hat{\theta}}_1 = -\sigma_1\hat{\theta}_1 + \frac{z_1^2 S_1(\underline{X}_1)^T S_1(\underline{X}_1)}{2a_1^2(k_{b1}^2 - z_1^2)^2} \tag{23}$$

where $c_1 > 0$ and $\sigma_1 > 0$ are the design constants.

Combing (21)-(23), it follows that

$$\dot{V}_1 \leqslant -c_1\frac{z_1^2}{k_{b1}^2 - z_1^2} + \frac{\varphi z_1 z_2}{k_{b1}^2 - z_1^2} + \sigma_1\tilde{\theta}_1\hat{\theta}_1 + \frac{\epsilon_1^2}{2} + \frac{a_1^2}{2} \tag{24}$$

Employing Young's inequality gives

$$\sigma_1\tilde{\theta}_1\hat{\theta}_1 \leqslant -\frac{\sigma_1}{2}\tilde{\theta}_1^2 + \frac{\sigma_1}{2}\theta_1^2 \tag{25}$$

And then, (24) can be derived as

$$\dot{V}_1 \leqslant -c_1\frac{z_1^2}{k_{b1}^2 - z_1^2} - \frac{\sigma_1}{2}\tilde{\theta}_1^2 + \frac{\varphi z_1 z_2}{k_{b1}^2 - z_1^2} + m_1 \tag{26}$$

where $m_1 = \frac{\epsilon_1^2}{2} + \frac{a_1^2}{2} + \frac{\sigma_1}{2}\theta_1^2$

Step 2: From (15), the time derivative of the error z_2 is

$$\dot{z}_2 = z_3 + \alpha_2 + f_2 + d_2 - \dot{\alpha}_1 \tag{27}$$

where

$$\dot{\alpha}_1 = \frac{\partial\alpha_1}{\partial x_1}\dot{x}_1 + \frac{\partial\alpha_1}{\partial y_d}\dot{y}_d + \frac{\partial\alpha_1}{\partial\dot{y}_d}\ddot{y}_d + \frac{\partial\alpha_1}{\partial\hat{\theta}_1}\dot{\hat{\theta}}_1 + \frac{\partial\alpha_1}{\partial\Phi_1}\dot{\Phi}$$

Selecting BLF V_2 as

$$V_2 = V_1 + \frac{1}{2}\log\frac{k_{b2}^2}{k_{b2}^2 - z_2^2} + \frac{1}{2}\tilde{\theta}_2^2 \tag{28}$$

where $k_{b2} = k_{c2} - Y_2$, z_2 is defined in a set $\mathbb{K}_2 = \{z_2 || z_2| < k_{b2}\}$, $\tilde{\theta}_2 = \theta_2 - \hat{\theta}_2$, and $\hat{\theta}_2$ is the estimation of θ_2.

Then, one obtains

$$\dot{V}_2 \leqslant \dot{V}_1 + \frac{z_2}{k_{b2}^2 - z_2^2}(z_3 + \alpha_2 + f_2 + d_2 - \dot{\alpha}_1) - \tilde{\theta}_2\dot{\hat{\theta}}_2 \tag{29}$$

Similar to (19), one can get

$$\begin{aligned} F_2(\underline{X}_2) &= f_2 + d_2 - \dot{\alpha}_1 + \frac{\varphi z_1(k_{b2}^2 - z_2^2)}{k_{b1}^2 - z_1^2} \\ &= W_2^T S_2(\underline{X}_2) + \varepsilon_2 \end{aligned} \tag{30}$$

where $\underline{X}_2 = [\underline{x}_2, \hat{\theta}_1, y_d, \dot{y}_d, \ddot{y}_d]^T$, $|\varepsilon_2| \leqslant \epsilon_2$, $\epsilon_2 > 0$ is a given accuracy.

Employing Young's inequality, one has

$$\begin{aligned} \frac{z_2 F_2(\underline{X}_2)}{k_{b2}^2 - z_2^2} \leqslant& \frac{z_2^2\theta_2 S_2(\underline{X}_2)^T S_2(\underline{X}_2)}{2a_2^2(k_{b2}^2 - z_2^2)^2} + \frac{a_2^2}{2} \\ &+ \frac{z_2^2}{2(k_{b2}^2 - z_2^2)^2} + \frac{\epsilon_2^2}{2} \end{aligned} \tag{31}$$

where $\theta_2 = ||W_2||^2$, and $a_2 > 0$ is a constant.

Combining (29) and (31) yields

$$\begin{aligned} \dot{V}_2 \leqslant& \dot{V}_1 + \frac{z_2}{k_{b2}^2 - z_2^2}\left(\alpha_2 + \frac{z_2\theta_2 S_2(\underline{X}_2)^T S_2(\underline{X}_2)}{2a_2^2(k_{b2}^2 - z_2^2)}\right. \\ &\left. + \frac{z_2}{2(k_{b2}^2 - z_2^2)}\right) + \frac{z_2 z_3}{k_{b2}^2 - z_2^2} + \frac{\epsilon_2^2}{2} + \frac{a_2^2}{2} \\ &- \frac{\varphi z_1 z_2}{k_{b1}^2 - z_1^2} - \tilde{\theta}_2\dot{\hat{\theta}}_2 \end{aligned} \tag{32}$$

Then, α_2 and $\hat{\theta}_2$ are designed as

$$\alpha_2 = -c_2 z_2 + \frac{z_2\hat{\theta}_2 S_2(\underline{X}_2)^T S_2(\underline{X}_2)}{2a_2^2(k_{b2}^2 - z_2^2)} + \frac{z_2}{2(k_{b2}^2 - z_2^2)} \tag{33}$$

$$\dot{\hat{\theta}}_2 = -\sigma_2\hat{\theta}_2 + \frac{z_2^2 S_2(\underline{X}_2)^T S_2(\underline{X}_2)}{2a_2^2(k_{b2}^2 - z_2^2)^2} \tag{34}$$

where $c_2 > 0$ and $\sigma_2 > 0$.

Combinating (32)-(34) produces

$$\begin{aligned}\dot{V}_2 \leqslant \dot{V}_1 - c_2\frac{z_2^2}{k_{b2}^2-z_2^2} + \frac{z_2 z_3}{k_{b2}^2-z_2^2} + \sigma_2\tilde{\theta}_2\hat{\theta}_2 \\ + \frac{\epsilon_2^2}{2} + \frac{a_2^2}{2} - \frac{\varphi z_1 z_2}{k_{b1}^2-z_1^2}\end{aligned} \tag{35}$$

And then, it yields

$$\begin{aligned}\dot{V}_2 \leqslant -c_1\frac{z_1^2}{k_{b1}^2-z_1^2} - \frac{\sigma_1}{2}\tilde{\theta}_1^2 - c_2\frac{z_2^2}{k_{b2}^2-z_2^2} - \frac{\sigma_2}{2}\tilde{\theta}_2^2 \\ + \frac{z_2 z_3}{k_{b2}^2-z_2^2} + m_2\end{aligned} \tag{36}$$

where $m_2 = \frac{\epsilon_2^2}{2} + \frac{a_2^2}{2} + \frac{\sigma_2}{2}\theta_2^2 + m_1$.

Step i: Noting that $z_i = x_i - \alpha_{i-1}$, we obtain

$$\dot{z}_i = z_{i+1} + \alpha_i + f_i + d_i - \dot{\alpha}_{i-1} \tag{37}$$

where $\dot{\alpha}_{i-1} = \sum_{j=1}^{i-1}\frac{\partial\alpha_{i-1}}{\partial x_j}\dot{x}_j + \sum_{j=0}^{i-1}\frac{\partial\alpha_{i-1}}{\partial y_d^{(j)}}y_d^{(j+1)} + \sum_{j=1}^{i-1}\frac{\partial\alpha_{i-1}}{\partial\hat{\theta}_j^{(j)}}\dot{\hat{\theta}}_j + \sum_{j=0}^{i-1}\frac{\partial\alpha_{i-1}}{\partial\Phi_j^{(j)}}\Phi^{(j+1)}$.

The BLF V_i is constructed as

$$V_i = V_{i-1} + \frac{1}{2}\log\frac{k_{bi}^2}{k_{bi}^2-z_i^2} + \frac{1}{2}\tilde{\theta}_i^2 \tag{38}$$

where $k_{bi} = k_{ci} - Y_i$, z_i is defined in a set $\mathbb{K}_i = \{z_i||z_i| < k_{bi}\}$, $\tilde{\theta}_i = \theta_i - \hat{\theta}_i$, and $\hat{\theta}_i$ is the estimation of θ_i.

Differentiating V_i gives

$$\dot{V}_i \leqslant \dot{V}_{i-1} + \frac{z_i}{k_{bi}^2-z_i^2}(z_{i+1} + \alpha_i + f_i + d_i - \dot{\alpha}_{i-1}) - \tilde{\theta}_i\dot{\hat{\theta}}_i \tag{39}$$

From Lemma 3, one can get

$$\begin{aligned}F_i(\underline{X}_i) &= f_i + d_i - \dot{\alpha}_{i-1} + \frac{z_{i-1}(k_{bi}^2-z_i^2)}{k_{bi-1}^2-z_{i-1}^2} \\ &= W_i^T S_i(\underline{X}_i) + \varepsilon_i\end{aligned} \tag{40}$$

where $\underline{X}_i = [\underline{x}_i, \hat{\theta}_1, \ldots, \hat{\theta}_{i-1}, y_d, \ldots, y_d^{(i)}]^T$, $|\varepsilon_i| \leqslant \epsilon_i$, $\epsilon_i > 0$ is a given accuracy.

Similar to (31), there has

$$\begin{aligned}\frac{z_i F_i(\underline{X}_i)}{k_{bi}^2-z_i^2} \leqslant \frac{z_i^2\theta_i S_i(\underline{X}_i)^T S_i(\underline{X}_i)}{2a_i^2(k_{bi}^2-z_i^2)^2} + \frac{a_i^2}{2} \\ + \frac{z_i^2}{2(k_{bi}^2-z_i^2)^2} + \frac{\epsilon_i^2}{2}\end{aligned} \tag{41}$$

where $\theta_2 = ||W_2||^2$, and $a_2 > 0$.

Thus, (39) is computed as

$$\begin{aligned}\dot{V}_i \leqslant \dot{V}_{i-1} + \frac{z_i}{k_{bi}^2-z_i^2}\left(\alpha_i + \frac{z_i\theta_i S_i(\underline{X}_i)^T S_i(\underline{X}_i)}{2a_i^2(k_{bi}^2-z_i^2)}\right. \\ \left. + \frac{z_i}{2(k_{bi}^2-z_i^2)}\right) + \frac{z_i z_{i+1}}{k_{bi}^2-z_i^2} + \frac{\epsilon_i^2}{2} + \frac{a_i^2}{2} \\ - \frac{z_{i-1}z_i}{k_{bi-1}^2-z_{i-1}^2} - \tilde{\theta}_i\dot{\hat{\theta}}_i\end{aligned} \tag{42}$$

Hence, α_i and $\hat{\theta}_i$ are designed as

$$\alpha_i = -c_i z_i + \frac{z_i\hat{\theta}_i S_i(\underline{X}_i)^T S_i(\underline{X}_i)}{2a_i^2(k_{bi}^2-z_i^2)} + \frac{z_i}{2(k_{bi}^2-z_i^2)} \tag{43}$$

$$\dot{\hat{\theta}}_i = -\sigma_i\hat{\theta}_i + \frac{z_i^2 S_i(\underline{X}_i)^T S_i(\underline{X}_i)}{2a_i^2(k_{bi}^2-z_i^2)^2} \tag{44}$$

where $c_i > 0$ and $\sigma_i > 0$.

Putting (43)-(44) into (42) gives

$$\begin{aligned}\dot{V}_i \leqslant \dot{V}_{i-1} - c_i\frac{z_i^2}{k_{bi}^2-z_i^2} + \frac{z_i z_{i+1}}{k_{bi}^2-z_i^2} + \sigma_2\tilde{\theta}_i\hat{\theta}_i + \frac{\epsilon_i^2}{2} \\ + \frac{a_i^2}{2} - \frac{z_{i-1}z_i}{k_{bi-1}^2-z_{i-1}^2}\end{aligned} \tag{45}$$

Simplifying (45) yields

$$\dot{V}_i \leqslant -\sum_{j=1}^{i} c_j\frac{z_j^2}{k_{bj}^2-z_j^2} - \sum_{j=1}^{i}\frac{\sigma_j}{2}\tilde{\theta}_j^2 + \frac{z_i z_{i+1}}{k_{bi}^2-z_i^2} + m_i \tag{46}$$

where $m_i = \frac{\epsilon_i^2}{2} + \frac{a_i^2}{2} + \frac{\sigma_i}{2}\theta_i^2 + m_{i-1}$.

Next, the ETC mechanism is established:

$$\begin{aligned}\varpi(t) = -(1+\lambda_1)\left(\alpha_n\tanh\left(\frac{z_n\alpha_n}{\kappa(k_{bn}^2-z_n^2)}\right)\right. \\ + \frac{\lambda_2}{1-\lambda_1}\tanh\left(\frac{z_n\lambda_2}{\kappa(1-\lambda_1)(k_{bn}^2-z_n^2)}\right) \\ \left. + \frac{\lambda_3\,\mathrm{sech}\left(\sum_{m=1}^{n}|z_m|\right)}{1-\lambda_1}\tanh\frac{z_n\lambda_3\,\mathrm{sech}\left(\sum_{m=1}^{n}|z_m|\right)}{\kappa(1-\lambda_1)(k_{bn}^2-z_n^2)}\right)\end{aligned} \tag{47}$$

$$\begin{aligned}u(t) &= \varpi(t_k), \forall t \in [t_k, t_{k+1}), \\ t_{k+1} &= \inf\left\{t \in \mathbb{R}^+ || e_T(t)| \geq \lambda_1|u(t)| + \lambda_2\right. \\ &\quad \left. + \lambda_3\,\mathrm{sech}\left(\sum_{m=1}^{n}|z_m|\right)\right\}\end{aligned} \tag{48}$$

where $e_T(t) = \varpi(t) - u(t)$, $0 < \lambda_1 < 1$, $\lambda_2 > 0, \lambda_3 > 0, \kappa > 0$, and $t_k (k \in \mathbb{N}^+, t_1 = 0)$ represents the update time.

Remark 3. In contrast to the methodology presented in [13], where the adaptive ETC strategy was defined as a strictly decreasing function involving the control of the tracking error and the input signal, the designed scheme does not require the introduction of additional parameters to prevent singularity. The introduction of the Hyperbolic Secant function (48) saves communication resources.

Invoking (47), (48) and Lemma 2, one can deduce that:

$$\begin{aligned}\frac{z_n\rho_a u(t)}{k_{bn}^2-z_n^2} \leqslant \rho_a\left(\frac{z_n\alpha_n}{k_{bn}^2-z_n^2} - \left|\frac{z_n\lambda_2}{(k_{bn}^2-z_n^2)(1-\lambda_1)}\right|\right. \\ - \left|\frac{z_n\lambda_3\,\mathrm{sech}\left(\sum_{m=1}^{n}z_m\right)}{(k_{bn}^2-z_n^2)(1-\lambda_1)}\right| + \frac{z_n\lambda_2}{(k_{bn}^2-z_n^2)(1-\lambda_1)} \\ \left. + \frac{z_n\lambda_3\,\mathrm{sech}\left(\sum_{m=1}^{n}z_m\right)}{(k_{bn}^2-z_n^2)(1-\lambda_1)} + 0.8355\kappa\right) \\ \leqslant \frac{z_n}{k_{bn}^2-z_n^2}\alpha_n + 0.8355\kappa\end{aligned} \tag{49}$$

Step n: Considering $z_n = x_n - \alpha_{n-1}$, there has

$$\dot{z}_n = \rho_a u + \psi + f_n + d_n - \dot{\alpha}_{n-1} \tag{50}$$

where $\dot{\alpha}_{n-1} = \sum_{j=1}^{n-1} \frac{\partial \alpha_{n-1}}{\partial x_j}\dot{x}_j + \sum_{j=0}^{n-1} \frac{\partial \alpha_{n-1}}{\partial y_d^{(j)}} y_d^{(j+1)} + \sum_{j=1}^{n-1} \frac{\partial \alpha_{n-1}}{\partial \hat{\theta}_j^{(j)}}\dot{\hat{\theta}}_j + \sum_{j=0}^{n-1} \frac{\partial \alpha_{n-1}}{\partial \Phi_j^{(j)}}\Phi^{(j+1)}$.

Structure the ultimate BLF as

$$V_n = V_{n-1} + \frac{1}{2}\log\frac{k_{bn}^2}{k_{bn}^2 - z_n^2} + \frac{1}{2}\tilde{\theta}_n^2 \tag{51}$$

where $k_{bn} = k_{cn} - Y_n$, $z_n \in \mathbb{K}_n$, and $\mathbb{K}_n = \{z_n || z_n| < k_{bn}\}$. $\tilde{\theta}_n = \theta_n - \hat{\theta}_n$, and $\hat{\theta}_n$ is the estimation of θ_n.

From (51), one obtains

$$\begin{aligned}\dot{V}_n \leqslant \dot{V}_{n-1} + \frac{z_n}{k_{bn}^2 - z_n^2}(\rho_a u + \psi + f_n + d_n - \dot{\alpha}_{n-1}) \\ - \tilde{\theta}_n\dot{\hat{\theta}}_n\end{aligned} \tag{52}$$

Similar to Step i

$$\begin{aligned}F_n(\underline{X}_n) &= \psi + f_n + d_n - \dot{\alpha}_{n-1} + \frac{z_{n-1}(k_{bn}^2 - z_n^2)}{k_{bn-1}^2 - z_{n-1}^2} \\ &= W_n^T S_n(\underline{X}_n) + \varepsilon_n\end{aligned} \tag{53}$$

where $\underline{X}_n = [\underline{x}_n, \hat{\theta}_n, \ldots, \hat{\theta}_{n-1}, y_d, \ldots, y_d^{(n)}]^T$, $|\varepsilon_n| \leqslant \epsilon_n$, $\epsilon_n > 0$ is a given accuracy.

Similar to (31), it produces

$$\begin{aligned}\frac{z_n F_n(\underline{X}_n)}{k_{bn}^2 - z_n^2} \leqslant &\frac{z_n^2\theta_n S_n(\underline{X}_n)^T S_n(\underline{X}_n)}{2a_n^2(k_{bn}^2 - z_n^2)^2} + \frac{a_n^2}{2} \\ &+ \frac{z_n^2}{2(k_{bn}^2 - z_n^2)^2} + \frac{\epsilon_n^2}{2}\end{aligned} \tag{54}$$

where $\theta_n = ||W_n||^2$, and $a_n > 0$.

Using (49), (52) and (54), it holds

$$\begin{aligned}\dot{V}_n \leqslant \dot{V}_{n-1} + \frac{z_n}{k_{bn}^2 - z_n^2}(\alpha_n + \frac{z_n\theta_n S_n(\underline{X}_n)^T S_n(\underline{X}_n)}{2a_n^2(k_{bn}^2 - z_n^2)} \\ + \frac{z_n}{2(k_{bn}^2 - z_n^2)}) + \frac{\epsilon_n^2}{2} + \frac{a_n^2}{2} - \frac{z_{n-1}z_n}{k_{bn-1}^2 - z_{n-1}^2} \\ - \tilde{\theta}_n\dot{\hat{\theta}}_n + 0.8355\kappa\end{aligned} \tag{55}$$

Construct α_n and $\hat{\theta}_n$ as

$$\alpha_n = -c_n z_n + \frac{z_n\hat{\theta}_n S_n(\underline{X}_n)^T S_n(\underline{X}_n)}{2a_n^2(k_{bn}^2 - z_n^2)} + \frac{z_n}{2(k_{bn}^2 - z_n^2)} \tag{56}$$

$$\dot{\hat{\theta}}_n = -\sigma_n\hat{\theta}_n + \frac{z_n^2 S_n(\underline{X}_n)^T S_n(\underline{X}_n)}{2a_n^2(k_{bn}^2 - z_n^2)^2} \tag{57}$$

where $c_n > 0$ and $\sigma_n > 0$.

Putting (56)-(57) into (55), one obtains

$$\dot{V}_n \leqslant -\sum_{j=1}^{n} c_j\frac{z_j^2}{k_{bj}^2 - z_j^2} - \sum_{j=1}^{n}\frac{\sigma_j}{2}\tilde{\theta}_j^2 + m_n + 0.8355\kappa \tag{58}$$

where $m_n = \frac{\epsilon_n^2}{2} + \frac{a_n^2}{2} + \frac{\sigma_n}{2}\theta_n^2 + m_{n-1}$.

From Lemma 4, (58) can be deduce that

$$\dot{V}_n \leqslant -CV_n + M \tag{59}$$

where $C = \min\{2c_j, \sigma_j, j = 1, \ldots, n\}$ and $M = \max\{m_n + 0.8355\kappa\}$.

Through the above design process, we have the following theorem.

Theorem 1. Considering the plant (1), the design of event-triggered prescribed time controller (48) can be achieved by designing the virtual controllers (23), (33), (43) and (56), as well as the adaptive laws (24), (34), (44) and (57), and collectively ensures the following:

1) Each signal is constrained within bounds, and the tracking error converges to a defined region within a prescribed time frame. The dimensions of both the small region and the prescribed time can be tailored by judiciously selecting the design parameters.

2) All states never cross the defined boundary, namely, $|x_i| < k_{c_i}$, $i = 1, 2, \ldots, n$.

3) The triggered interval time $t_{k+1} - t_k \geq t_*$, indication of non-occurrence of Zeno behavior.

Proof: By multiplying e^{Ct} both sides of (59), we get

$$\frac{d\left(e^{Ct}V_n(t)\right)}{dt} \leqslant Me^{Ct} \tag{60}$$

Integrating (60) yields

$$V_n \leqslant V_n(0)e^{-Ct} + \frac{M}{C} \tag{61}$$

Then, taking (51) and (61), one gets

$$z_i \leqslant \sqrt{2V_n(0)e^{-Ct} + \frac{2M}{C}}, i = 1, 2, \ldots, n. \tag{62}$$

Followed it, $\tilde{\theta}_i$ is also bounded. From (11)-(13) and Lemma 1, we have $-T_1\Phi(t) < e(t) < T_2\Phi(t)$ in the prescribed-time T_s. Noting that $z_i < k_{bi}$ and y_d, α_i is clearly bounded. Due to the definition of e, it is true that $|x_1| < |z_1| + |y_d| < k_{b1} + Y_1$. Since $k_{b1} = k_{c1} - Y_1$, thus, it has $|x_1| < k_{c_1}$. Further, we can obtain that α_1 is bounded, that is, $|\alpha_1| < Y_2$, and combining $x_2 = z_2 + \alpha_1$ shows $|x_2| < k_{b2} + Y_2$, then $|x_2| < k_{c2}$. Similarly, it is easy to verify $|x_i| < k_{ci}$, $i = 3, \ldots, n$.

With respect to (48), we then obtain

$$\dot{e}_T(t) = \dot{\varpi}(t) - \dot{u}(t) = \dot{\varpi}(t) \tag{63}$$

using the fact that $|\dot{\varpi}(t)| < \varpi^*$, and $\varpi^* > 0$ is a constant. Then, we obtain

$$e_T(t_{k+1}) - e_T(t_k) = \dot{e}_T(t)(t_{k+1} - t_k) \tag{64}$$

where $t \in (t_k, t_{k+1})$.

Solving for $e_T(t_k) = 0$ and $\lim_{t\to t_{k+1}} e_T(t) = \lambda_1|u(t)| + \lambda_3\,\mathrm{sech}\left(\sum_{m=1}^{n} z_m\right) + \lambda_2$ reveal $t_* \geqslant \frac{\lambda_2}{\varpi^*}$, hence, the event-triggered is Zeno-free. The proof is completed.

IV. SIMULATION

To validate the proposed method, A physical example is given by the following equation [7]

$$\begin{cases}\dot{x}_1 = x_2 + d_1, \\ \dot{x}_2 = \frac{1}{M_m}\left(-k_0 x_1 e^{-x_1} - h_d x_2^2 + u^F\right) + d_2, \\ y = x_1\end{cases} \tag{65}$$

where $M_m = 1$ and $h_d = 1.1$ are the mass of the cart and the damping factor, respectively. The reference trajectory is $y_d = \sin(t)$. $d_1(t) = 0.1\cos(0.5t)$ and $d_2(t) = 0.2\sin(t)$ represent bounded external disturbances. The state constraints are

$|x_1| < k_{c1} = 1.6$ and $|x_2| < k_{c2} = 2 + 4.8e^{-t}$. Furthermore, we set u^F as

$$u^F = \begin{cases} u(t), & 0 \leqslant t \leqslant 15 \\ \rho_a(t)u(t) + \psi(t), & t > 15 \end{cases} \tag{66}$$

where $\rho_a(t) = 0.6$, $\psi(t) = 2\sin(2t)$.

The control algorithm are designed as

$$\begin{aligned}
\alpha_1 =& -\frac{1}{\varphi}\left(c_1 z_1 + \frac{z_1 \hat{\theta}_1 S_1(\underline{X}_1)^T S_1(\underline{X}_1)}{2a_1^2(k_{b1}^2 - z_1^2)} + \frac{z_1}{2(k_{b1}^2 - z_1^2)}\right) \\
\alpha_2 =& -c_2 z_2 + \frac{z_2 \hat{\theta}_2 S_2(\underline{X}_2)^T S_2(\underline{X}_2)}{2a_2^2(k_{b2}^2 - z_2^2)} + \frac{z_2}{2(k_{b2}^2 - z_2^2)} \\
\varpi(t) =& -(1+\lambda_1)\left(\alpha_n \tanh\left(\frac{z_n \alpha_n}{\kappa(k_{bn}^2 - z_n^2)}\right)\right. \\
&+ \frac{\lambda_2}{1-\lambda_1}\tanh\left(\frac{z_n \lambda_2}{\kappa(1-\lambda_1)(k_{bn}^2 - z_n^2)}\right) \\
&\left.+ \frac{\lambda_3 \operatorname{sech}\left(\sum_{m=1}^n z_m\right)}{1-\lambda_1}\tanh\frac{z_n \lambda_3 \operatorname{sech}\left(\sum_{m=1}^n z_m\right)}{\kappa(1-\lambda_1)(k_{bn}^2 - z_n^2)}\right) \\
\dot{\hat{\theta}}_1 =& -\sigma_1 \hat{\theta}_1 + \frac{z_1^2 S_1(\underline{X}_1)^T S_1(\underline{X}_1)}{2a_1^2(k_{b1}^2 - z_1^2)^2} \\
\dot{\hat{\theta}}_2 =& -\sigma_2 \hat{\theta}_2 + \frac{z_2^2 S_2(\underline{X}_2)^T S_2(\underline{X}_2)}{2a_2^2(k_{b2}^2 - z_2^2)^2}
\end{aligned} \tag{67}$$

The relevant parameters are chosen as $a_1 = a_2 = 8$, $c_1 = 16$, $c_2 = 18$, $\sigma_1 = 8$, $\sigma_2 = 5$, $k_{b1} = 1.6$, $k_{b2} = 1.2$, $\lambda_1 = 0.3$, $\lambda_2 = 0.6$, $\lambda_3 = 0.5$, and $\kappa = 1.8$. The initials are set as $[x_1(0), x_2(0), \hat{\theta}_1(0), \hat{\theta}_2(0)]^T = [-0.5, 0.1, 0.4, 0.3]^T$. In addition, the prescribed-time control parameters are set as $T_s = 2$, $\nu_1 = 1$, $\nu_2 = 0.2$, and $T_1 = T_2 = 0.9$.

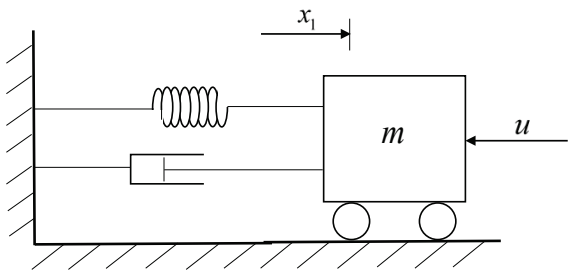

Fig. 1. Mass-spring-damper system.

Remark 4. Fig. 3 illustrates the successful implementation of prescribed-time control. With a specified convergence time set at 2s, the tracking error not only effectively converges but also achieves stability within this defined time frame. After 15 seconds, the impact of the actuator fault on the system becomes apparent, as illustrated in Fig. 6. Remarkably, despite the fault, Fig. 2 demonstrates that the system output effectively tracks the reference signal. This shows that our control scheme is robust against disturbances.

Remark 5. Diverging from the ETC techniques introduced in [11] and [23], the approach presented in this paper incorporates a diminishing function to set a more substantial triggering threshold. Comparative simulation results are outlined in Fig. 8. Furthermore, the designed control scheme is adept at addressing scenarios involving actuator failure,

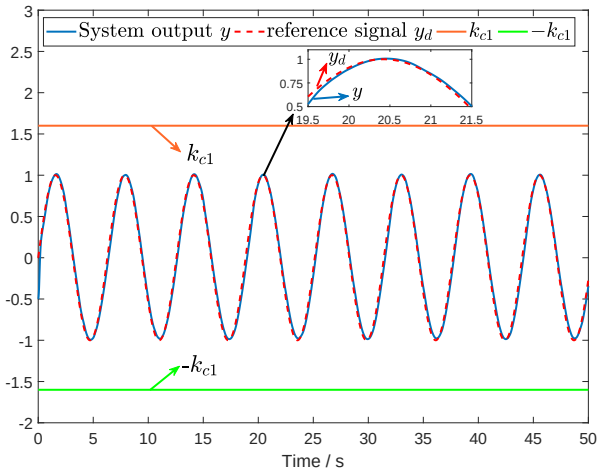

Fig. 2. Trajectories of the desired signal y_d, output y, and its constraint condition.

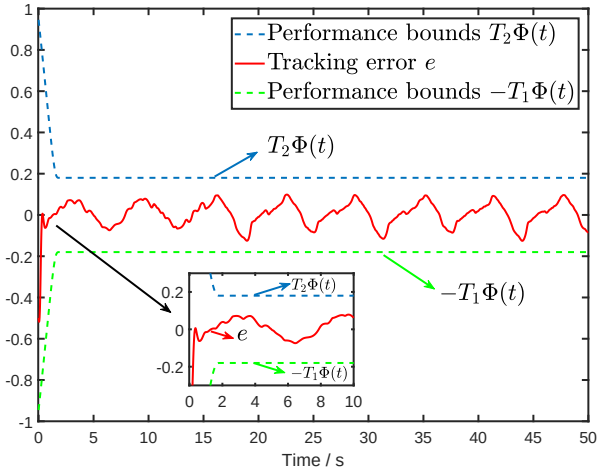

Fig. 3. Tracking performance.

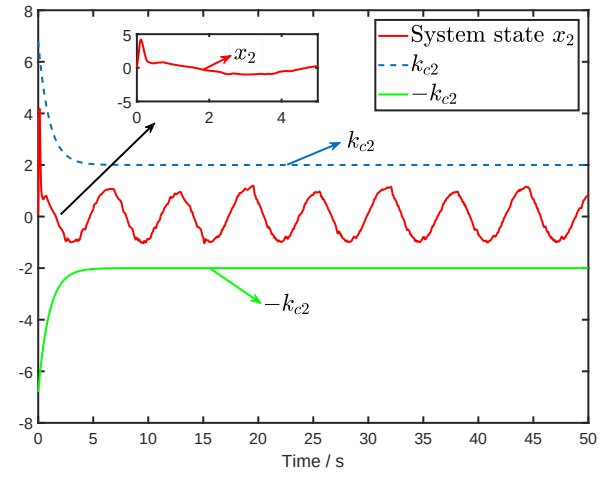

Fig. 4. Trajectories of system state x_2 and its constraint condition.

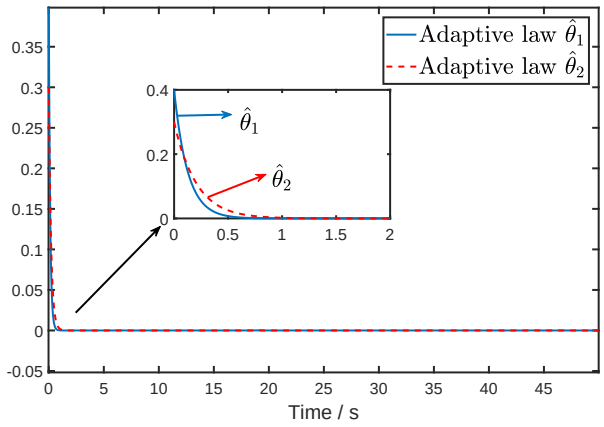

Fig. 5. Response curves of adaptive laws.

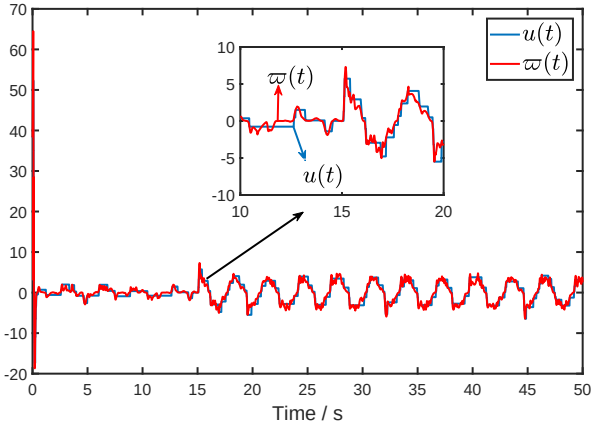

Fig. 6. Input signals of the event-triggered control $u(t)$ and the continuous control $\varpi(t)$.

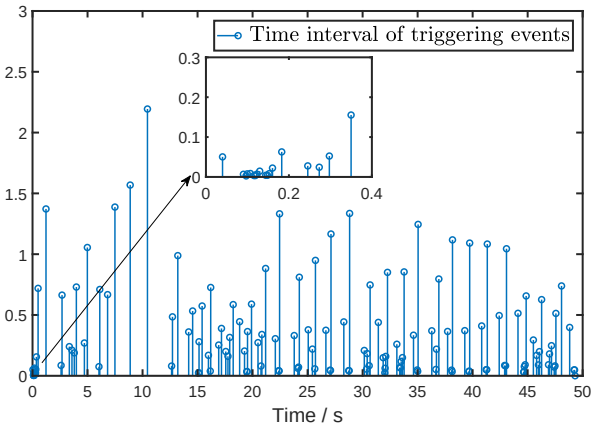

Fig. 7. Time interval of event-triggered.

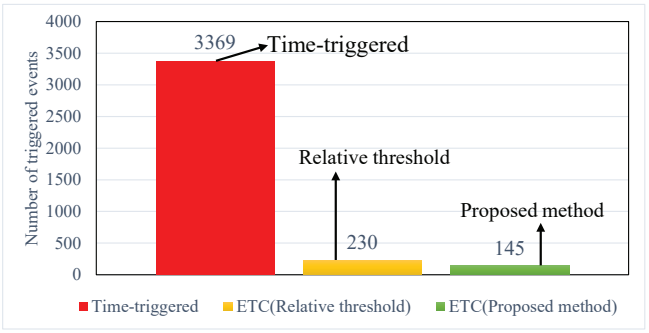

Fig. 8. The number of triggered events.

effectively mitigating the impact on the system. Both features contribute to the heightened practical utility of the proposed method in industrial control applications.

V. CONCLUSION

The problem of adaptive prescribed-time event-triggered fault-tolerant control of a special class of nonlinear systems under actuator failure and full-state constraints is investigated in this paper. The designed scheme , integrating backstepping techniques and BLF, introduces an adaptive prescribed-time ETC mechanism that surpasses conventional ETC methods. Remarkably, it not only reduces the number of triggering instances but also significantly shortens the convergence time. Moreover, this scheme ensures the compliance of all system states with constraints, maintaining bounded signals within the system. Additionally, We also demonstrate that the tracking error converges to the designated region $(-T_1\Phi(t), T_2\Phi(t))$ within the prescribed time. The future work aims to extend this approach to more complex output feedback nonlinear systems.

REFERENCES

[1] M. Krstic, I. Kanellakopoulos, and P. V. Kokotovic, "Nonlinear and adaptive control design," New York: Wiley, 1995.

[2] L. Ma, and L. Liu, "Adaptive neural network control design for uncertain nonstrict feedback nonlinear system with state constraints , " *IEEE Transactions on Systems, Man, and Cybernetics: Systems*, vol. 51, no. 6, pp. 3678-3686, 2021.

[3] Y. Ma, N. Zhao, X. Ouyang, H. Xu, and Y. Zhou, "Adaptive fuzzy prescribed performance control for strict-feedback stochastic nonlinear system with input constraint," *Engineering Letters*, vol. 29, no. 2, pp. 650-657, 2021.

[4] M. Wang, Z. Wang, H. Dong, and Q. Han, "A novel framework for backstepping-based control of discrete-time strict-feedback nonlinear systems with multiplicative noises," *IEEE Transactions on Automatic Control*, vol. 66, no. 4, pp. 1484-1496, 2021.

[5] Z. Li, Y. Wei, and L. Wang, "Active event-triggered fault-tolerant control design for switched pure-feedback nonlinear systems," *Engineering Letters*, vol. 31, no. 3, pp. 896-905, 2023.

[6] H. Wang, K. Xu, and J. Qiu, "Event-triggered adaptive fuzzy fixed-time tracking control for a class of

nonstrict-feedback nonlinear systems," *IEEE Transactions on Circuits and Systems I: Regular Papers*, vol. 68, no. 7, pp. 3058-3068, 2021.

[7] Y. Liu, Q. Zhu, and N. Zhao, "Event-triggered adaptive fuzzy control for switched nonlinear systems with state constraints," *Information Sciences* vol. 562, pp. 28-43, 2021.

[8] Q. Zhang and D. He, "Adaptive fuzzy sliding exact tracking control based on high-order log-type time-varying BLFs for highorder nonlinear systems," *IEEE Transactions on Fuzzy Systems*, vol. 31, no. 1, pp. 14-24, 2023.

[9] Z. Xu, C. Gao, and H. Jiang, "High-gain-observer-based output feedback adaptive controller design with command filter and event-triggered strategy," *IAENG International Journal of Applied Mathematics*, vol. 53, no. 2, pp. 463-469, 2023.

[10] Y. Zang, N. Zhao, X. Ouyang, and J. Zhao, "Prescribed performance adaptive control for nonlinear systems with unmodeled dynamics via event-triggered," *Engineering Letters*, vol. 31, no. 4, pp. 1770-1779, 2023.

[11] L. Xing, C. Wen, Z. Liu, H. Su, and J. Cai, "Event-triggered adaptive control for a class of uncertain nonlinear systems," *IEEE Transactions on Automatic Control*, vol. 62, no. 4, pp. 2071-2076, 2017.

[12] W. Sun, S. Su, Y. Wu, and J. Xia, "Adaptive fuzzy event-triggered control for high-order nonlinear systems with prescribed performance," *IEEE Transactions on Cybernetics*, vol. 52, no. 5, pp. 2885-2895, 2022.

[13] L. Wu, J. H. Park, X. Xie, C. Gao, and N. Zhao, "Fuzzy adaptive event-triggered control for a class of uncertain nonaffine nonlinear systems with full state constraints," *IEEE Transactions on Fuzzy Systems*, vol. 29, no. 4, pp. 904-916, 2020.

[14] J. Zhao, X. Ouyang, N. Zhao, and Y. Zang, "Fixed-time fuzzy adaptive control for switched nonlinear systems with input constraints based on event-triggered," *IAENG International Journal of Computer Science*, vol. 50, no. 4, pp. 1431-1439, 2023.

[15] Q. Yu, X. He, L. Wu, and L. Guo, "Finite-time command filtered event-triggered adaptive output feedback control for nonlinear systems with unknown dead-zone constraints," *Information Sciences*, vol. 617, pp. 482-497, 2022.

[16] W. Li and M. Krstic, "Prescribed-time output-feedback control of stochastic nonlinear systems," *IEEE Transactions on Automatic Control*, vol. 68, no. 3, pp. 1431-1446, 2023.

[17] C. Hua, P. Ning, and K. Li, "Adaptive prescribed-time control for a class of uncertain nonlinear systems," *IEEE Transactions on Automatic Control*, vol. 67, no. 11, pp. 6159-6166, 2022.

[18] Y. Salmanpour, M. M. Arefi, A. Khayatian, and S. Yin, "Observer-based fault-tolerant finite-time control of nonlinear multiagent systems," *IEEE Transactions on Neural Networks and Learning Systems*, to be published.

[19] S. Yin, H. Yang, and O. Kaynak, "Sliding mode observer-based FTC for Markovian jump systems with actuator and sensor faults," *IEEE Transactions on Automatic Control*, vol. 62, no. 7, pp. 3551-3558, 2017.

[20] L. Wu, J. H. Park, and N. Zhao, "Robust adaptive fault-tolerant tracking control for nonaffine stochastic nonlinear systems with full-state constraints," *IEEE Transactions on Cybernetics*, vol. 50, no. 8, pp. 3793-3805, 2019.

[21] L. Wu and J. Park, "Adaptive fault-tolerant control of uncertain switched nonaffine nonlinear systems with actuator faults and time delays," *IEEE Transactions on Systems, Man, and Cybernetics: Systems*, vol. 50, no. 9, pp. 3470-3480, 2020.

[22] Y. Liu, H. Zhang, Y. Wang, H. Ren and Q. Li, "Adaptive fuzzy prescribed finite-time tracking control for nonlinear system with unknown control directions," *IEEE Transactions on Fuzzy Systems*, vol. 30, no. 6, pp. 1993-2003, 2022.

[23] J. Wang, Q. Gong, K. Huang, Z. Liu, C. Philip Chen, and J. Liu, "Event-triggered prescribed settling time consensus compensation control for a class of uncertain nonlinear systems with actuator failures," *IEEE Transactions on Neural Networks and Learning Systems*, vol. 34, no. 9, pp. 5590-5600, 2023.